NAL TR-392T

UDC 533.27:
533.6.011.5:
661.96

# TECHNICAL REPORT OF NATIONAL AEROSPACE LABORATORY

## TR-392T

## On Turbulent Diffusion in Coaxial Jets of Dissimilar Gases with Pressure Gradient

Shigeaki NOMURA

October 1974

NATIONAL AEROSPACE LABORATORY

CHŌFU, TOKYO, JAPAN

# On Turbulent Diffusion in Coaxial Jets of Dissimilar Gases with Pressure Gradient *

Shigeaki NOMURA**


## 概　　要

異種気体から成る超音速同軸ジェットの乱流拡散を，軸方向に圧力勾配のある場合について，理論的に取扱かった。乱流の平均量に対する伴流方程式を線型化して求めたLibbyとKleinstein の解析解を検討し，この解が圧力勾配のある流れ場でも，粒子拡散に対しては適用できる事を示し，これを用いて乱流拡散係数に対するモデル式を与えた。このモデル化した乱流拡散係数を用いて伴流方程式を数値的に解き，代表的実験例との比較を行なった。その結果，圧力勾配のない場合については，速度，粒子密度の半径方向，軸方向分布のいずれについても良い一致が得られた。軸方向圧力勾配のある場合には，粒子密度，温度の軸方向分布について良い一致が得られた。速度分布については，$Sc_t$ を定数で与えているため実験との一致が得られず，乱流シュミット数（又は Eddy 粘性係数）に対する圧力勾配を含んだ適当なモデル化が今後の問題として提起された。

## SUMMARY

Focusing the attention upon the field with the axial pressure gradient, the turbulent diffusion in the coaxial jets of dissimilar gases has been investigated theoretically. Dealing with the mean values of the turbulent flow, the turbulent diffusion coefficient has been modeled by means of employing the solutions for the linearized species equation as obtained by Libby and Kleinstein.

The turbulent wake equations involving this new diffusion model have been solved numerically. Comparing these solutions with the existing experimental results, the following conclusions are drawn;

(1) For the jet mixing without the pressure gradient, the present diffusion model provides excellent predictions of axial and radial profiles both for concentration and velocity.

(2) For the case with large axial pressure gradient, the axial profile of concentration and temperature could be predicted satisfactorily, however, the velocity profile could not.

(3) Though $Sc_t$, $Pr_t$ and $Le_t$ have been proved to be constant throughout the mixing field without pressure gradient, $Sc_t$ has been found not to be constant for the case with pressure gradient.


## NOMENCLATURE

| | |
|---|---|
| $Cp$ | Specific heat at constant pressure |
| $\overline{Cp}$ | Normalized specific heat with respect to $Cp_e$ |
| $\overline{Cp_k}$ | Normalized specific heat of the $k^{\text{th}}$ gas; $k$ = 1 corresponds to inner jet gas and $k$=2 to outer jet gas |
| $D_j$ | Inner jet nozzle diameter |
| $D_t$ | Turbulent diffusion coefficient |
| $H$ | Total enthalpy of gas |
| $h$ | Static enthalpy of gas |

* Received January 14, 1974; This work has been conducted under the supervision of Prof. V. Zakkay when the author stayed at the Aerospace Lab. of New York Univ., U.S.A.. The author wishes to acknowledge Dr. V. Zakkay and Dr. R. Sinha for their good suggestions and discussions.

** First Aerodynamics Division.

$Le_t$ Turbulent Lewis number
$M$ Local Mach number
$n$ Concentration decay exponent along the center line
$p$ Static pressure
$Pr_t$ Turbulent Prandtl number
$R$ Gas constant
$Re$ Reynolds number
$r$ Radial coordinate
$r_j$ Radius of the inner jet nozzle
$r_{mc}$ Concentration half radius defined such that $Y_j = Y_{j\mathcal{L}}/2$ at $r = r_{mc}$
$\overline{r_{mc}}$ Normalized half radius with respect to $r_j$
$Sc_t$ Turbulent Schmidt number
$T$ Temperature
$\overline{T}$ Normalized temperature with respect to $T_e$
$u$ Axial velocity component
$\overline{u}$ Normalized axial velocity with respect to $u_e$
$v$ Radial velocity component
$x$ Axial coordinate
$x_i$ Initial value of $x$ to start computation
$x_o$ Concentration potential core length
$\overline{x}$ Normalized axial coordinate with respect to $r_j$
$\tilde{x}$ Normalized axial coordinate with respect to $x_o$
$Y_j$ Mass concentration of inner jet gas
$Y_k$ Mass concentration of $k^{th}$ gas; $k = 1$ corresponds to inner jet gass, and $k = 2$ to outer jet gas
$\zeta$ Transformed axial coordinate defined as $\frac{1}{4}\int_{\bar{x}_i}^{\bar{x}} Re^{-1}\, d\bar{x}$
$\epsilon$ Eddy viscosity
$\gamma$ Specific heat ratio
$\lambda$ Mass flow ratio defined as $\rho_j u_j / \rho_e u_e$
$\Psi$ Modified stream function defined by eq. (7) or $\left(\int_0^{\bar{r}} \overline{\rho u}\, \bar{r}\, d\bar{r}\right)^{1/2}$
$\phi_{u\mathcal{L}}$ Normalized centerline velocity defined by $(u_e - u_{\mathcal{L}})/(u_e - u_{ji})$
$\xi$ Transformed axial coordinate defined as $2\int_0^{\bar{x}} \overline{(\rho D_t)}_{\bar{x},0}\, d\bar{x}$
$\rho$ Density
$\tau_t$ Turbulent shear stress
$\mu_t$ Turbulent viscosity
$(\overline{\rho D_t})$ Normalized value of $\rho D_t$ with respect to $\rho_j u_j r_j$
$(\overline{\rho u})$ Normalized value of $\rho u$ with respect to $\rho_j u_j$
$(\overline{\rho v})$ Normalized value of $\rho v$ with respect to $\rho_j u_j$

Subscript

$\mathcal{L}$ Centerline value
$e, \infty$ External free stream condition
$i$ Initial condition
$j$ Inner jet condition

## 1. INTRODUCTION

The turbulent mixing problem of the coaxial jet of variable density has been an area of considerable interest and ever increasing practical importance in the past decade, as opposed to the constant density mixing whose investigations can be traced back to the 1930's.

This problem is related, practically, to the mixing of fuel and oxidizer gas in the combustion chambers of Ram and Scram jet engines, to the flow in the exhaust plume from rockets, and the like. Furthermore, the recent interest in the supersonic combustion jet engines has dictated the extensive works for the mixing of high speed coaxial jets composed of the dissimilar gases.

This problem, however, has not been solved satisfactorily yet, mainly because the enough informations have not been obtained for the dependence of the turbulent transport coefficients on the flow properties, especially in the presence of pressure gradient in the flow field.

Therefore, it is the purpose of this report to investigate theoretically the high speed jet mixing with pressure gradient, and to determine the dependence of these transport properties on the flow properties.

Concerning the transport properties in the compressible flow, the main efforts have been focused on finding the proper expression for the turbulent shear stress $\tau_t$ which is assumed to be given by $\tau_t = \rho\varepsilon \cdot (\partial u/\partial y)$ in analogy to a laminar flow. In Ref. 1 Ferri extended the Prandtl's eddy viscosity model for the constant density flow to the variable density flow. However, as pointed out in Ref. 2, this model fails when the mass flux of each stream is equal.

Ting-Libby[3] determined the compressibility factor for the Prandtl's model using their transformation, while Donaldson[4] and Peters[5] obtained the compressibility factor empirically. These models, however, fail also when the velocity of each stream is equal, since the Prandtl's model becomes zero. In Ref. 6 Zakkay et al. developed the eddy viscosity model in terms of the centerline velocity and the velocity half radius, which has been shown not to be valid for general cases by Chriss[12]. Schetz[7] extended Clauser's[8] model to the axisymmetric wake which was expressed in terms of the mass deffect across the wake. The eddy viscosity models above mentioned are as follows;

Prandtl ; $\mu_t = \kappa_P \rho \gamma_{mu} \left| u_\ell - u_e \right|$

Ferri ; $\mu_t = \kappa_F \gamma_{m\rho u} \left| (\rho u)_\ell - (\rho u)_e \right|$

Ting–Libby ; $\mu_t = (\mu_t)_{\text{Prandtl}} \cdot (\rho_e / \rho)^2 / \gamma^2 \cdot \int_0^\gamma 2\gamma \, \rho / \rho_e \cdot d\gamma$

Donaldson & Peters ; $\mu_t = (\mu_t)_{\text{Prandtl}} \cdot \{0.66 + 0.34 \exp(-3.42 M_{mu}^2)\}$

Zakkay ; $\mu_t = \kappa_Z \rho_\ell \gamma_{mu} u_\ell$

Schetz ; $\mu_t = \kappa_S / \gamma_j \int_0^\infty \left| \rho u - \rho_e u_e \right| \gamma \, d\gamma$

As seen in this table each of all these models has a constant $\kappa$ which should be chosen such that the numerical solutions of wake equations with the proposed eddy viscosity and appropriate constant values for $Pr_t$ and $Sc_t$ agree with the experimental data. Therefore, it has been found in Refs. 2, 9, 10, and 12 that though all these models provide good predictions for certain very restricted flow conditions, none of them is valid for the general case.

Comparing with these numerous works for the eddy viscosity, only few works have been done for another transport properties, namely $Pr_t$, $Sc_t$, and $Le_t$. In the analytical and numerical investigations, so far, the constant values of $Pr_t$ and $Sc_t$ have been assumed and the several experimental studies seem to approve these assumptions of constant properties under the condition of zero pressure gradient in the mixing flow field.

In Ref. 11 Forstal and Shapillow determined $Le_t = 1.0$ and $Pr_t = Sc_t = 0.7$ using the data of air to air mixing measured at very low speed. Zakkay et al.[6] carried out extensive measurements in the turbulent mixing of high speed coaxial jets comprised of several dissimilar gases. For hydrogen and air mixing $Sc_t = 0.8 \sim 2.0$ and $Le_t = 0.9 \sim 1.2$ have been concluded. Chriss[12] measured very detailed profiles in mixing of high speed coaxial air and hydrogen jets, and $Le_t = 1.0$ has been obtained. The accuracy of this Chriss's experimental data has been checked by Zelanzny et al.[9] and Harsha[10] by means of "Constant Momentum Integral Check" and were found to be excellent. Peters, Chriss, and Paulk[13] have shown, for one case of hydrogen and air mixing given in Ref. 12, that $Pr_t = Sc_t = 0.85$ is approximately valid which consequently means $Le_t = 1.0$. Zelanzny et al.[9] also calculated $Sc_t$ for four cases of Chriss' data and confirmed the results obtained by Peters et al. .

Though there is considerable scatter in these reported transport coefficients calculated by the inverse solution of wake equations using the measured flow properties, the constant values for $Pr_t$, $Sc_t$, and $Le_t$ seem to be valid under the condition that the pressure gradient is negligible in the mixing field.

As opposed to the mixing with zero pressure gradient, only the following information is avairable for the mixing with the finite pressure gradient; the experimental observations reported in Refs. 6, 14, 15 and 24 that the behavior of mass diffusion is not affected by the pressure gradient significantly, while the momentum transfer is affected definitely. This fact suggests that the diffusion coefficient, if modeled appropriately, will give the proper prediction for, at least, the mass diffusion in the mixing flow field with pressure gradient.

Under these circumstances the turbulent diffusion coefficient is modeled for the coaxial jet mixing of the dissimilar gases with pressure gradient, assuming the constant $Pr_t$, $Sc_t$, and $Le_t$. The numerical solutions of wake equations are carried out for the both cases with and without pressure gradient to investigate the validity of the diffusion model presented herein.

## 2. THEORETICAL ANALYSIS

### 2-1. Modeling of Turbulent Diffusion Coefficient

The governing equations for the mean turbulent flow properties in the coaxial jet mixing with the axial pressure gradient can be described as follows[1, 16];

Conservation of Mass

$$\frac{\partial}{\partial x}(\rho u) + \frac{1}{r}\frac{\partial}{\partial r}(\rho v r) = 0 \qquad (1)$$

Conservation of Momentum

$$\rho u \frac{\partial u}{\partial x} + \rho v \frac{\partial u}{\partial r} = \frac{1}{r} \frac{\partial}{\partial r} \left( \rho \varepsilon r \frac{\partial u}{\partial r} \right) - \frac{dp}{dx} \tag{2}$$

Conservation of Energy

$$\rho u \frac{\partial H}{\partial x} + \rho v \frac{\partial H}{\partial r} = u \frac{dp}{dx} + \frac{1}{r} \frac{\partial}{\partial r} \left[ \frac{\rho \varepsilon}{Pr_t} r \frac{\partial H}{\partial r} + \frac{Pr_t - 1}{Pr_t} \cdot \rho \varepsilon r u \frac{\partial u}{\partial r} + \frac{Le_t - 1}{Pr_t} \cdot \rho \varepsilon r \sum_k h_k \frac{\partial Y_k}{\partial r} \right] \tag{3}$$

Conservation of Species

$$\rho u \frac{\partial Y_j}{\partial x} + \rho v \frac{\partial Y_j}{\partial r} = \frac{1}{r} \frac{\partial}{\partial r} \left( \frac{\rho \varepsilon}{Sc_t} r \frac{\partial Y_j}{\partial r} \right),$$

$$\mu_t = \rho \varepsilon, \; D_t = \frac{\varepsilon}{Sc_t} \tag{4}$$

where the following conditions were assumed;

(1) the flow is chemically frozen

(2) the radial pressure gradient is not existing

(3) the streamwise pressure gradient may exist and therefore, the external flow conditions could be variable.

In Refs. 16 and 17 these eqs. (1)~(4) are solved for the axisymmetric coaxial jet mixing with the assumptions of $dp/dx = 0$, of $Pr_t = Sc_t = Le_t = 1.0$ and of the initial step profiles for velocity, enthalpy, and concentration. Obviously these assumptions reduce those equations to a single equation and then the solution can be applicable for any flow properties. As for these assumptions, however, the transport coefficients $Pr_t$, $Sc_t$ and $Le_t$ could not generally be equal to unity, and the initial profiles have not always step profiles due to the boundary layers developed on the jet nozzle wall. The only one exact application of this solution is possible for the species equation together with the appropriately modeled turbulent diffusion coefficient which excludes $Sc_t$ from eq. (4) as seen in eq. (5), since the initial profile for species is always a step type ($Y_j = 1.0$ for $r \leq r_j$, $Y_j = 0$ for $r > r_j$). Furthermore, even if the axial pressure gradients existed, the mass diffusion will not be affected as mentioned previously; this can be seen also from the basic equations where the pressure gradient affects only indirectly the concentration through velocity and temperature field. Therefore, the solution for the wake equation obtained in Refs. 16 and 17 with the assumptions of $dp/dx = 0$, of $Pr_t = Le_t = Sc_t = 1.0$ and of the initial step profiles, can be applied correctly to the species equation together with the turbulent diffusion coefficient in the mixing field with the axial pressure gradient.

The species equation with the diffusion coefficient is

$$\rho u \frac{\partial Y_j}{\partial x} + \rho v \frac{\partial Y_j}{\partial r} = \frac{1}{r} \frac{\partial}{\partial r} \left( \rho D_t r \frac{\partial Y_j}{\partial r} \right) \tag{5}$$

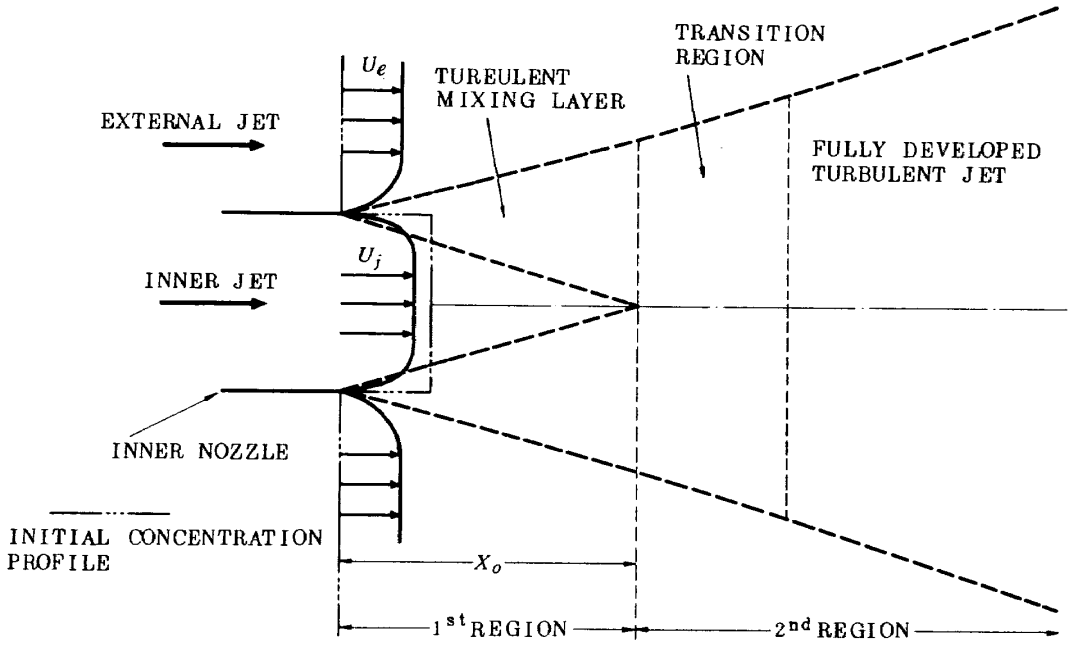


Fig. 1 Turbulent Jet Mixing Flow Model

with

initial conditions at $x = 0$

$Y_j = 1$ for $0 \leq r \leq r_j$

$Y_j = 0$ for $r_j < r < \infty$

boundary conditions

$\partial Y_j/\partial r = 0$ at $r = 0$

$Y_j = 0$ at $r \to \infty$

Employing the same method as Kleinstein, who obtained the solution for the linearized wake equation by the application of the modified von Mises transformation in Ref. 17, the species equation can be solved as follows; Eq. (5) is transformed to

$$\frac{\partial Y_j}{\partial \bar{x}} = \frac{4}{\Psi}\frac{\partial}{\partial \Psi}\left[\overline{(\rho D_t)}\ \overline{(\rho u)}\ \bar{r}^2\left(\frac{1}{\Psi}\frac{\partial Y_j}{\partial \Psi}\right)\right] \quad (6)$$

by the transformation of

$$\bar{x} = x/r_j,\ \frac{\partial}{\partial \bar{r}}\left(\frac{\Psi}{2}\right)^2 = \overline{(\rho u)}\cdot\bar{r},\ \frac{\partial}{\partial \bar{x}}\left(\frac{\Psi}{2}\right)^2 = -\overline{(\rho v)}\cdot\bar{r} \quad (7)$$

where $\overline{(\ )}$ shown in NOMENCLATURE.

Neglecting the fourth order term in the Taylor series expanded form of

$$\left[\overline{(\rho D_t)}\ \overline{(\rho u)}\ \bar{r}^2\right]_{\bar{x},\Psi} = \left[\overline{(\rho D_t)}\right]_{\bar{x},0}\cdot\Psi^2/2 + 0(\Psi^4)$$

the species equation (6) reduces to the linear form in the $(\xi, \Psi)$ plane as

$$\frac{\partial Y_j}{\partial \xi} = \frac{1}{\Psi}\frac{\partial}{\partial \Psi}\left(\Psi\frac{\partial Y_j}{\partial \Psi}\right) \quad (7a)$$

where $\xi$ was defined by $\xi = 2\int_0^{\bar{x}} \overline{(\rho D_t)}_{\bar{x},0}\, d\bar{x}$

Assuming the initial step profile such that $Y_j = Y_{j\ell}$ for $0 \leq \Psi \leq \Psi_j$ and $Y_j = 0$ for $\Psi > \Psi_j$, the solution of this well known heat conduction equation can be expressed along the centerline by

$$Y_{j\ell} = 1 - \exp(-\Psi_j^2/4\xi) \quad (8)$$

where $\Psi_j = 2\left[\int_0^1 \overline{\rho u}\ \bar{r}\, d\bar{r}\right]^{1/2}_{\text{nozzle exit}} = \sqrt{2}$

Solving eq. (7a), Masters showed that in the far wake region of $\xi \to \infty$, $Y_j/Y_{j\ell}$ approaches the Gaussian distribution[23] as

$$Y_j/Y_{j\ell} = \exp(-\Psi^2/4\xi) \quad (9)$$

This asymptotic solution can be used to introduce the diffusion model together with eq. (8).

Since $(\overline{\rho u}) \to 1/\lambda$ in the far wake region of $\xi \to \infty$,

$$\Psi^2 = 2\bar{r}^2/\lambda$$

and

$$Y_j/Y_{j\ell} = \exp(-\bar{r}^2/2\lambda\xi) \quad (10)$$

are resulted.

In addition to these relations, the empirical law for the centerline concentration decay of $Y_{j\ell} = \tilde{x}^{-n} \equiv (x/x_0)^{-n}$ is to be used here which relation was pointed out by Zakkay et al.[6, 14, 15, 24] and was confirmed by Chriss[12].

Eliminating $\xi$ from eqs. (8) and (10) with the substitution of the above empirical relation for $Y_{j\ell}$, the concentration profile can be expressed in the physical plane as

$$Y_j = \tilde{x}^{-n}(1 - \tilde{x}^{-n})^{\bar{r}^2/\lambda} \quad (11)$$

Also the asymptotic jet spread expressed in terms of the half radius of concentration $r_{mc}$ can be drawn from eq. (11) with $Y_{j\ell} = \tilde{x}^{-n}$ as

$$\lim_{x\to\infty}\bar{r}_{mc} = \lim_{x\to\infty}\left[\frac{\lambda \ln(Y_j/Y_{j\ell})}{\ln(1-\tilde{x}^{-n})}\right]^{1/2}_{Y_j = Y_{j\ell}/2} = \left[\ln 2\lambda\tilde{x}^{-n}\right]^{1/2} = 0.833\left[\lambda(x/x_0)^n\right]^{1/2} \quad (12)$$

This may provide an analytical prediction of the concentration half radius.

Once the concentration profile was expressed in the physical plane by eq. (11), the turbulent diffusion coefficient can be derived from the species equation inversely.

The species eq. (5) is described with the aid of continuity equation by

$$\rho D_t\, r\frac{\partial Y_j}{\partial r} = \int_0^r \frac{\partial(\rho u Y_j)}{\partial x} r'\, dr' - Y_j\int_0^r r'\frac{\partial(\rho u)}{\partial x}\, dr'$$

Then the diffusion coefficient along the centerline can be expressed as *

---

* $$(\rho D_t)_{\ell} = \lim_{r\to 0}\rho D_t = \lim_{r\to 0}\left[\left\{\int_0^r \frac{\partial(\rho u Y_j)}{\partial x} r' dr' - Y_j\int_0^r r'\frac{\partial(\rho u)}{\partial x}\, dr'\right\}\Big/\left(r\frac{\partial Y_j}{\partial r}\right)\right]$$

$$= \lim_{r\to 0}\left[\left\{\frac{\partial(\rho u Y_j)}{\partial x} r - Y_j r\frac{\partial(\rho u)}{\partial x} - \frac{\partial Y_j}{\partial r}\int_0^r r'\frac{\partial(\rho u)}{\partial x}\, dr'\right\}\Big/\left(\frac{\partial Y_j}{\partial r} + r\frac{\partial^2 Y_j}{\partial r^2}\right)\right] \to \text{eq.} \quad (13)$$

where $(\partial Y_j/\partial r)_{\ell} = 0$ by axisymmetric condition.

$$(\rho D_t)_{\ell} = \left[\rho u \frac{\partial Y_j}{\partial x} \Big/ \left(2 \frac{\partial^2 Y_j}{\partial r^2}\right)\right]_{\ell} \qquad (13)$$

Substituting eq. (11) into eq. (13) the turbulent diffusion coefficient on the centerline becomes

$$(\rho D_t)_{\ell} = \frac{n r_j}{4 \overline{x_0}} \left(\frac{\overline{r}_{mc}^2}{\ln 2}\right)^{(1-1/n)} \cdot \lambda^{1/n} (\rho u)_{\ell} \qquad (14)$$

In eq. (14) there are two unknown parameters, namely $\overline{x_o}$ and $n$. The decay exponent $n$ has been shown as

$$n = 2 \quad \{ \text{ in } Y_{j\ell} = x^{-n} \} \qquad (15)$$

for high speed jet mixing in many experiments[6,14,15,24].

Now the potential core length $\overline{x_o}$ for concentration in the high speed mixing where $n = 2$ is valid, should be formulated in terms of known values.

Rearranging the existing experimental data, it has been found that the momentum ratio of two jets at the initial exit plane is the important parameter for the potential core length for concentration. The typical correlation between the potential core length for concentration and the initial Mach number ratio can be seen obviously in Fig. 2 for which the flow conditions are shown in Table 1. The Mach number ratio of two jets can be expressed by the momentum ratio as

$$\rho_j u_j^2 / \rho_e u_e^2 = (p u^2/RT)_j / (p u^2/RT)_e \sim (M_j/M_e)^2$$

since $p_j = p_e$. Therefore, Fig. 2 shows that when the momentum ratio becomes larger, the potential core length becomes longer.

These data are rearranged in Fig. 3, from which the correlation equation has been obtained as

$$\left(\frac{x_0}{D_j}\right)_{\substack{\text{concen-}\\ \text{tration}}} = 1 + 30 \left(\frac{\rho_j}{\rho_e}\right)^{1/4} M_j^2 \cdot \left[1 + M_j^2 \exp\left\{-\left(\frac{M_e}{M_j} - 1\right)^2/2\right\}\right]^{-2} \qquad (16)^*$$

From this equation one can get

$$(x_0/D_j)_{\text{concentration}} = 1.0 \quad \text{as} \quad M_j = 0$$

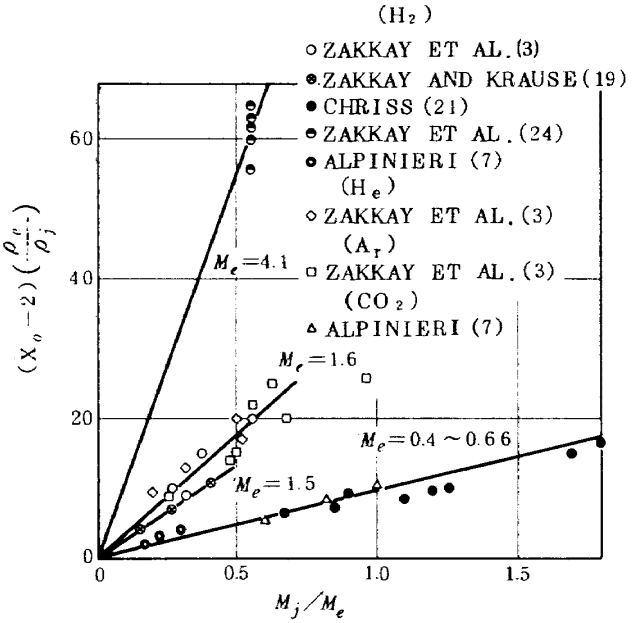


Fig. 2 Length of Concentration Potential Core vs. Mach Number Ratio

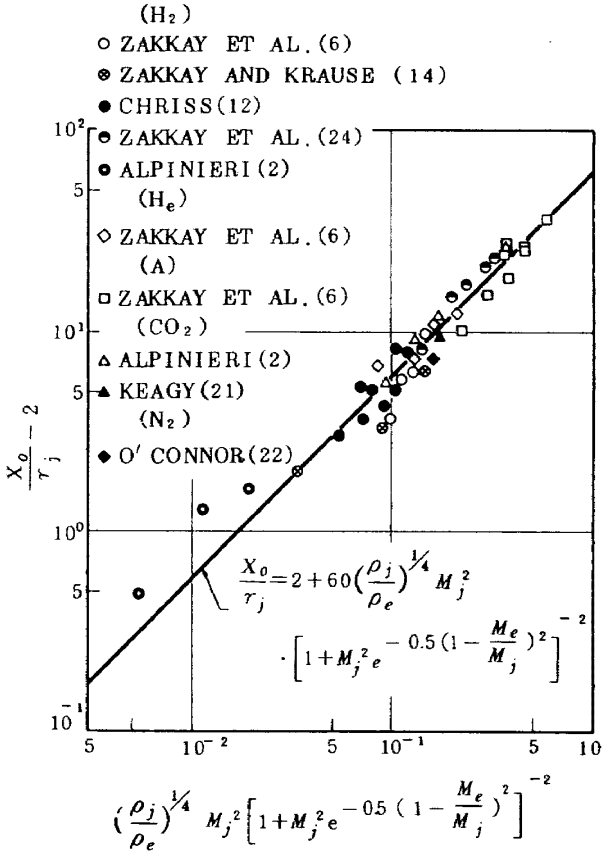


Fig. 3 Correlation for the Length of Concentration Potential Core

* This correlation equation has been determined from Fig. 2 with conditions of $x_o/D_j \doteqdot 1.0$ for $M_j = 0$ and of the data by Keagy and O'Connor for $M_e = 0$. The final optimum form was determined by using the graphic display of electric computer.

**Table 1 Experimental Data**

| Investigator | Gas | | $r_j$ | $u_j$ | $u_e$ | $\lambda$ | $\overline{x_O}$) | $M_j$ | $M_e$ | $T_j$ | $T_e$ |
|---|---|---|---|---|---|---|---|---|---|---|---|
| | Inner | Outer | in. | ft/sec | ft/sec | | concentration | | | °R | °R |
| Zakkay et al.[6] | $H_2$ | Air | 0.15 | 1930 | 2520 | 0.107 | 7.8 | 0.43 | 1.6 | 580 | 972 |
| | " | " | " | 1980 | 1360 | 0.047 | 5.2 | 0.51 | " | 500 | 366 |
| | " | " | " | 2300 | 1360 | 0.072 | 8.2 | 0.60 | " | 490 | " |
| | " | " | " | 3290 | 1360 | 0.124 | 11.5 | 0.89 | " | 460 | " |
| | He | " | " | 1150 | 2520 | 0.154 | 8.9 | 0.33 | " | 580 | 972 |
| | " | " | " | 2770 | 2520 | 0.288 | 14.0 | 0.87 | " | 480 | " |
| | " | " | " | 1490 | 1360 | 0.103 | 8.5 | 0.51 | " | 485 | 366 |
| | " | " | " | 2270 | 1360 | 0.185 | 13.1 | 0.82 | " | 440 | " |
| | Ar | " | " | 456 | 2520 | 0.497 | 12.2 | 0.42 | " | 566 | 972 |
| | " | " | " | 780 | 2520 | 1.07 | 20.0 | 0.77 | " | 500 | " |
| | " | " | " | 1090 | 2520 | 1.86 | 28.0 | 1.17 | " | 410 | " |
| | " | " | " | 1300 | 2520 | 2.97 | 38.0 | 1.61 | " | 330 | " |
| | " | " | " | 720 | 1360 | 0.59 | 17.0 | 0.82 | " | 517 | 366 |
| | " | " | " | 760 | 1360 | 0.79 | 25.0 | 0.89 | " | 506 | " |
| | " | " | 0.15 | 840 | 1360 | 0.98 | 30.0 | 1.00 | 1.6 | 488 | " |
| Chriss[12] | $H_2$ | " | 0.25 | 3300 | 528 | 0.56 | 9.8 | 0.79 | 0.42 | 486 | 630 |
| | " | " | " | 3200 | 735 | 0.39 | 6.8 | 0.77 | 0.61 | 490 | 600 |
| | " | " | " | 3050 | 792 | 0.32 | 6.0 | 0.73 | 0.66 | 495 | " |
| | " | " | " | 2400 | 792 | 0.24 | 5.5 | 0.56 | 0.56 | 516 | " |
| | " | " | " | 1900 | 797 | 0.19 | 5.0 | 0.44 | 0.66 | 530 | " |
| | " | " | " | 3100 | 682 | 0.62 | 10.5 | 0.74 | 0.44 | 500 | 1010 |
| | " | " | " | 2450 | 760 | 0.41 | 7.2 | 0.58 | 0.49 | 510 | 1000 |
| | " | " | " | 1950 | 780 | 0.30 | 7.3 | 0.45 | 0.50 | 530 | 1000 |
| | Air | " | 0.25 | 940 | 596 | 3.60 | 16.0* | 0.22 | 0.32 | 545 | 640 |
| Keagy & Weller[21] | $CO_2$ | " | 0.064 | 400 | 0 | $\infty$ | 11.3 | 0.51 | 0 | 392 | 420 |
| O'Conner et al.[22] | $N_2$** | " | 0.38 | 3750 | 0 | $\infty$ | 8.7 | 0.94 | 0 | 7700 | 420 |
| Eggers | Air | " | " | 1765 | 0 | $\infty$ | 25.0* | 2.2 | 0 | 265 | 520 |
| Donaldson[4] | $N_2$ | " | " | 2040 | 0 | $\infty$ | 35.3 | 3.3 | 0 | 152 | 520 |
| | " | " | " | 750 | " | " | 9.5 | 0.75 | " | 410 | " |
| | $CH_4$ | " | " | 2700 | " | " | 30.0 | 3.1 | " | 190 | " |
| | " | " | " | 940 | " | " | 8.43 | 0.75 | " | 390 | " |
| | $CO_2$ | " | " | 600 | " | " | 11.0 | 0.75 | " | 401 | " |
| Peters et al.[13] | Air*** | " | " | 405 | 49 | 7.8 | 11.0 | 0.35 | 0.04 | 556 | 530 |
| | " | " | " | 400 | 192 | 1.85 | 16.5 | 0.34 | 0.17 | 552 | 510 |
| | " | " | " | 405 | 263 | 1.35 | 17.0 | 0.35 | 0.24 | 552 | 505 |
| | " | " | " | 395 | 386 | 0.89 | 17.0 | 0.36 | 0.36 | 517 | 473 |
| | " | " | " | 380 | 485 | 0.68 | 14.5 | 0.33 | 0.46 | 528 | 465 |
| | " | " | " | 380 | 575 | 0.59 | 7.7 | 0.33 | 0.55 | 523 | 450 |
| Zakkay[14] | $H_2$ | " | 0.3 | 460 | 2300 | 0.022 | 1.8 | 0.11 | 1.55 | 518 | 945 |
| | " | " | " | 960 | " | 0.052 | 4.0 | 0.235 | " | 515 | " |
| | " | " | " | 1740 | " | 0.094 | 5.3 | 0.425 | " | 503 | " |
| | " | " | " | 2620 | " | 0.140 | 8.1 | 0.645 | " | 480 | " |
| Alpinieri[2] | $CO_2$ | " | 1.0 | 312 | 650 | 0.66 | 7.2 | 0.38 | 0.625 | " | 448 |
| | " | " | " | 422 | " | 0.95 | 11.0 | 0.51 | " | 471 | " |
| | " | " | " | 506 | " | 1.17 | 13.5 | 0.62 | " | 464 | " |
| Zakkay et al.[24] | $H_2$ | " | 0.3 | 6800 | 2200 | 0.07 | 24 | 2.25 | 4.1 | 250 | 120 |
| | " | " | " | | " | 0.016 | 10 | " | " | | " |
| | " | " | " | | " | 0.03 | 17 | " | " | | " |
| | " | " | " | | " | 0.044 | 20 | " | " | | " |
| | " | " | " | | " | 0.078 | 28 | " | " | | " |

* Potential Core Length for Velocity

** Partially Ionized Nitrogen Gas

*** Air with Small Amount of Hydrogen as Tracer Gas

which corresponds to the axisymmetric wake, and the result of $x_0/D_j \doteqdot 1.0$ is supported by the data of the supersonic wake studies[18,19,20]. When $M_e = 0$ which corresponds to the jet injected into the quiescent atmosphere, the data of Keagy[21] and O'Connor[22] are fairely well correlated as seen in this figure.

Now the diffusion coefficient of eq. (14) can be described, with the aid of eq. (15), as

$$\rho D_t = 0.6 \frac{\lambda^{1/2}}{\overline{x_0}} r_{mc} (\rho u)_{\ell} \qquad (17)^{**}$$

assuming that $\rho D_t$ is only the function of $x$.

It should be emphasized here that eq. (17) does not include any adjustable constant to match the numerical solutions of wake equations with the experimental data, which is included in all previous viscosity models proposed by Prandtl, Ferri, Schetz, Zakkay, and so forth.

### 2-2. Numerical Solutions of Wake Equations

The wake equations in the general form are written in the modified von Mises plane as follows;

Momentum equation

$$\frac{\partial \bar{u}}{\partial \zeta} = \frac{1}{\Psi}\frac{\partial}{\partial \Psi}\left(\frac{\bar{\rho}\,\bar{\mu}_t\,\bar{u}\,\bar{r}^2}{\Psi}\cdot\frac{\partial \bar{u}}{\partial \Psi}\right) - \frac{\bar{u}}{u_e}\frac{\partial u_e}{\partial \zeta}\left(1-\frac{1}{\bar{\rho}\,\bar{u}^2}\right)$$

Energy equation

$$\frac{\partial \bar{T}}{\partial \zeta} = \frac{1}{\Psi \bar{c}_p}\frac{\partial}{\partial \Psi}\left(\frac{\bar{\rho}\,\bar{\mu}_t\,\bar{c}_p\,\bar{u}\,\bar{r}^2}{P_{r_t}\,\Psi}\frac{\partial \bar{T}}{\partial \Psi}\right) + (\gamma_e - 1)M_e^2\left[\frac{\bar{T}-1}{\bar{\rho}\,\bar{c}_p\,u_e}\frac{\partial u_e}{\partial \zeta} + \frac{\bar{\rho}\,\bar{\mu}_t\,\bar{r}^2\bar{u}}{\bar{c}_p\,\Psi^2}\cdot\left(\frac{\partial \bar{u}}{\partial \Psi}\right)^2\right] + \frac{\bar{\rho}\,\bar{\mu}_t\,\bar{r}^2\,\bar{u}}{S_{c_t}\,\bar{c}_p\,\Psi^2}\frac{\partial \bar{T}}{\partial \Psi}\sum_k \bar{c}_{p\,k}\frac{\partial Y_k}{\partial \Psi}$$

Species equation

$$\frac{\partial Y_k}{\partial \zeta} = \frac{1}{\Psi}\frac{\partial}{\partial \Psi}\left(\frac{\bar{\rho}\,\bar{\mu}_t\,\bar{u}\,\bar{r}^2}{S_{c_t}\,\Psi}\cdot\frac{\partial Y_k}{\partial \Psi}\right) \quad k = 1, 2, \cdots N$$

where the modified von Mises transformation is defined by

$$\partial \Psi^2/\partial \bar{r} = \bar{\rho}\,\bar{u}\,\bar{r}\ ,\quad \partial \Psi^2/\partial \bar{x} = -\bar{\rho}\,\bar{v}\,\bar{r}\ ,$$

$$\zeta = 1/4 \cdot \int_{\bar{x}_i}^{\bar{x}} (Re)_e^{-1}\, d\bar{x}$$

and

$$\mu_t = Sc_t\,\rho D_t\ ,\quad Pr_t = Le_t \cdot Sc_t$$

are used.

The associated initial and boundary conditions are

$\bar{u}(0, \Psi) = \bar{u}_i(\Psi)$, $\bar{T}(0, \Psi) = \bar{T}_i(\Psi)$, $Y_j(0, \Psi) = Y_{ji}(\Psi)$,

$$\frac{\partial}{\partial \Psi}\bar{u}(\zeta, 0) = \frac{\partial}{\partial \Psi}\bar{T}(\zeta, 0) = \frac{\partial}{\partial \Psi}Y_j(\zeta, 0) = 0$$

$$\lim_{\Psi\to\infty}\bar{u}(\zeta, \Psi) = \lim_{\Psi\to\infty}\bar{T}(\zeta, \Psi) = 1.0,\ \lim_{\Psi\to\infty}Y_j(\zeta, \Psi) = 0$$

Since the transformed equations become parabolic, there is no difficulty for carrying out the numerical calculations by means of the fully implicit finite-difference scheme.

Once initial and boundary conditions are specified, these equations can be solved with the aid of eq. (17) for the diffusion coefficient and with the assumptions of appropriate constant values for $Sc_t$ and $Pr_t$. Throughout this present calculations, $Sc_t = Pr_t = 0.8$ ($Le_t = 1.0$) have been used.

In order to investigate the validity of the present diffusion model, the numerical calculations were started first for the cases without pressure gradient; the experimental data refered are from Chriss[12] and Alpinieri[2].

In Figs. 4 (a-1,2, b-1,2,3, c-1,2) the numerical solutions marched down from the initial profiles taken from the data of Chriss[12] which were the cases of hydrogen and air mixing are shown comparing with Chriss's experimental results. The accuracy of those experiments has been found to be very good by Zelanzny[9] and Harsha[10] (reportedly within 4%). Since the lateral profiles measured at several stations of $x$ were reported in Ref. 12, the initial profiles for this numerical calculations were chosen at the position of $\overline{x_i}$ indicated in figures instead of the assumed profiles at the jet exit plane. It should be noticed that these data showed the considerable thickness of boundary layer developed on the nozzle wall at the exit.

---

** For the numerical calculation the concentration half radius $r_{mc}$ should be determined by the numerical procedure instead of eq. (12) which will provide the analytical prediction of the half radius in the far wake region.

Fig. 4 (a-1, b-1, c-1) show the excellent agreement of numerical solutions with the experimental data for the concentration decay on the centerline and for the concentration half radius. Fig. 4 (b-3) shows an example for the lateral concentration profiles which agree quite well with the experimental data. This shows the validity of the assumption that $\rho D_t$ does not vary laterally accross the mixing region. Also in Figs. 4 (a-1, b-1 and c-1) the analytical predictions of concentration half radius $r_{mc}$ given by eq. (12) are

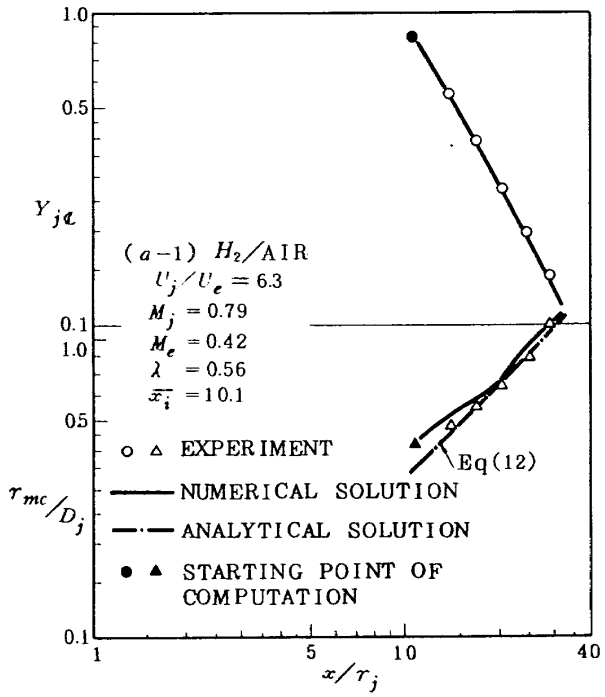


Fig. 4 (a-1) Comparison of Numerical Results with the Data of Chriss

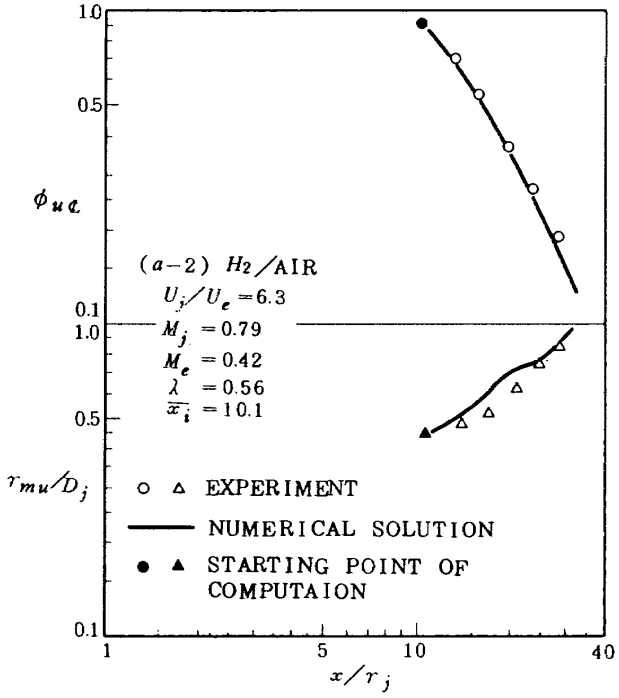


Fig. 4 (a-2)

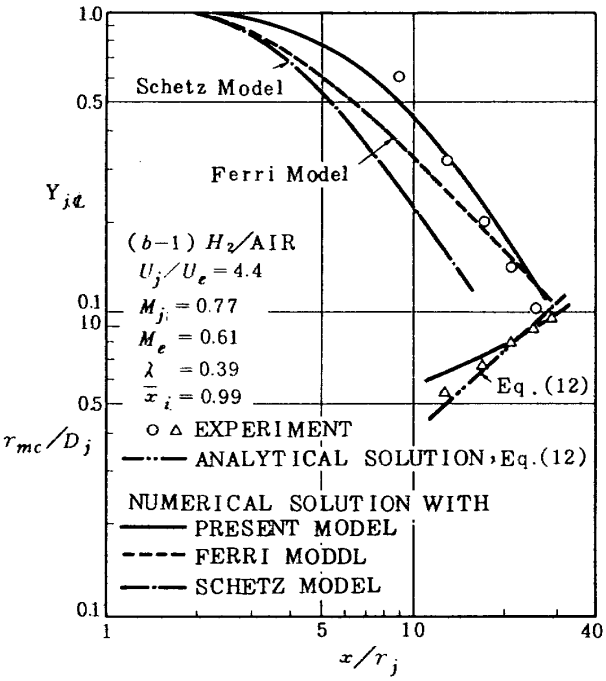


Fig. 4 (b-1)

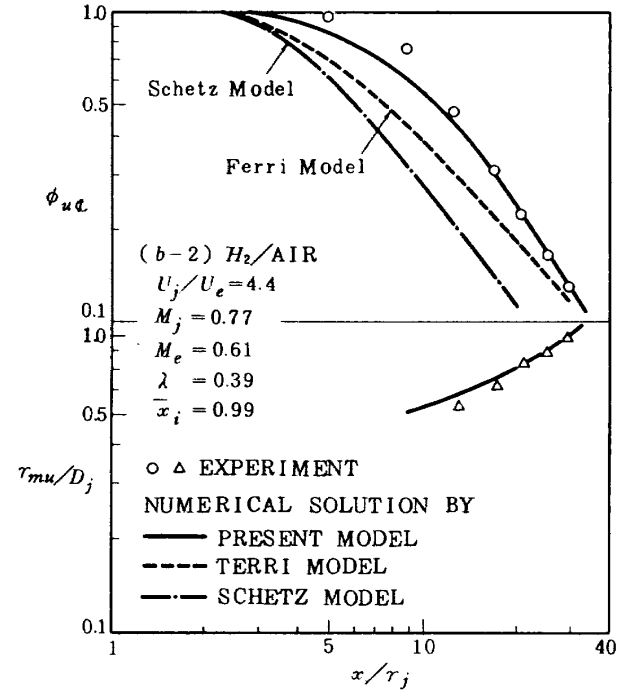


Fig. 4 (b-2)

shown. The agreement with the experimental data is excellent, considering that eq. (12) does not include any proportional constant to match the solutions with data.

Concerning the velocity profiles for the data of Chriss, the centerline profile and the half radius have been predicted well as seen in Figs. 4 (a-2, b-2 and c-2). These results proove that if there is no pressure

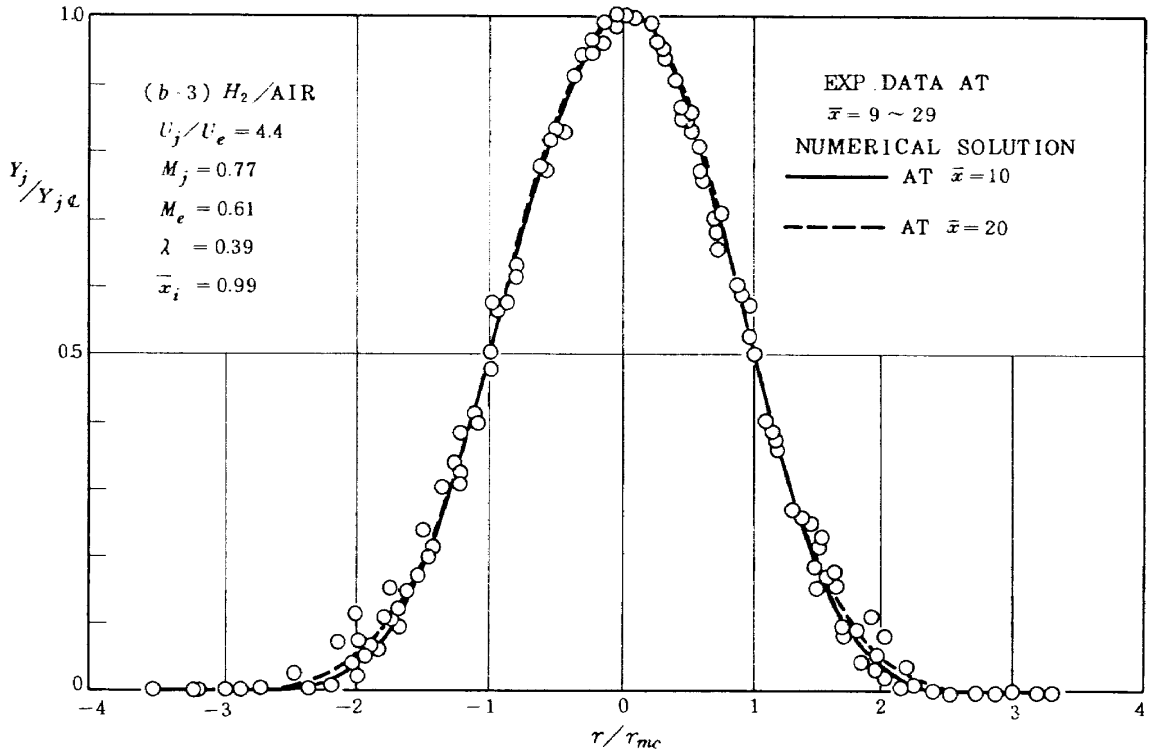


Fig. 4 (b-3)

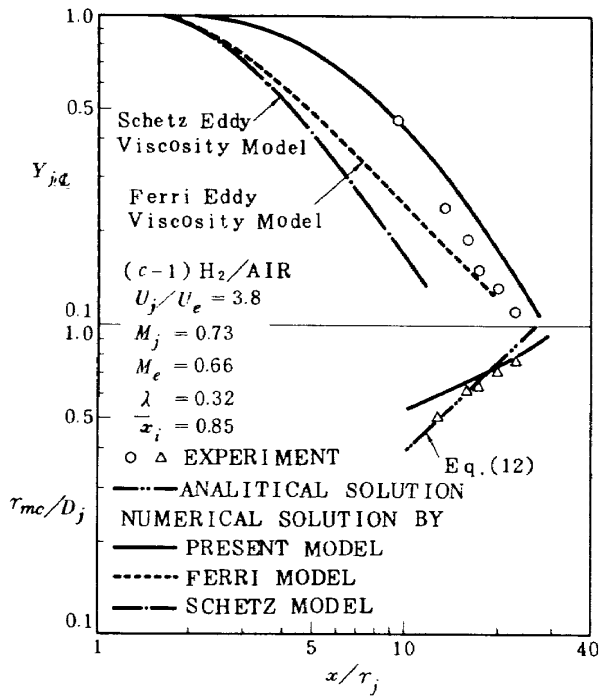


Fig. 4 (c-1)

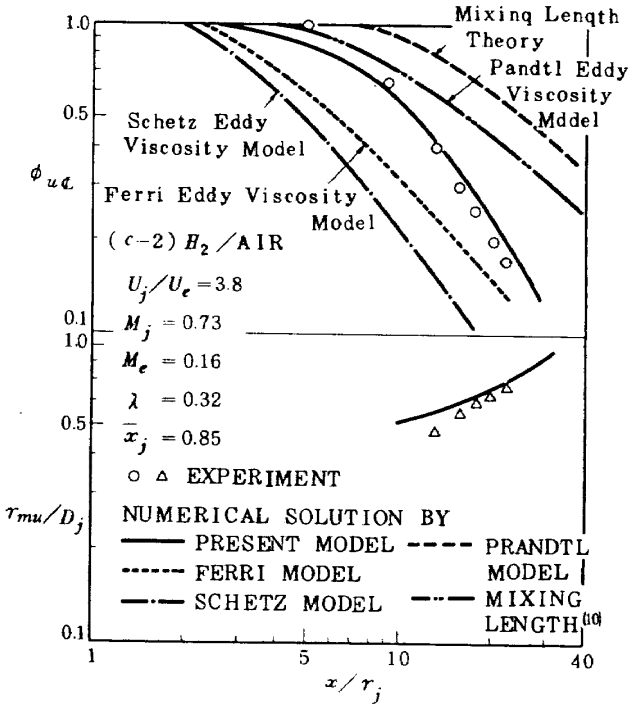


Fig. 4 (c-2)

gradient in the flow field the assumptions of $Sc_t$ = $Pr_t$ = 0.8 and $Le_t$ = 1.0 are appropriate for the high speed mixing of hydrogen and air.

In Figs. 4 (b-1 and c-1) the numerical solutions calculated by employing eddy viscosity models of Ferri[1] and Schetz[7] are presented also. The comparisons with the data indicate that the Ferri model provides fairly good predictions in the far wake region, but that Schetz model gives too fast decay for both cases.

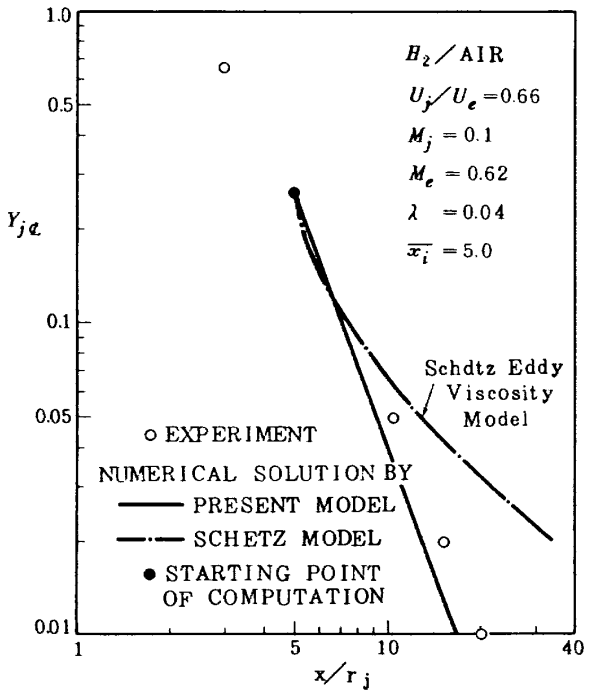


Fig. 5 Comparison of Numerical Results with the Data of Alpinieri(2)

The numerical result for the data of Alpinieri which are characterized by the very small momentum of the inner hydrogen jet is presented in Fig. 5. The result given by the present diffusion model agrees fairly well with the data. In the same figure the result given by Schetz model is shown, which does not predict even the decay trend correctly.

Throughout these numerical computations the momentum integral of the wake has been checked at each station of finite difference calculation and found to be constant with the accuracy of less than 1%.

Now the wake equations are solved for the case with the pressure gradient; the experimental data are taken from Ref. 24. The numerical procedures are the same except for obtaining the axial pressure distribution from measurements. As shown in Fig. 6 the smoothed profile was used for the simplisity in the computation, though the actual static pressure along the centerline is oscillating. This oscillation may stem from the weak under expansion of the inner jet as discussed in the following section. The numerical calculations were marched down from $x = 0$ with the experimental data until $x = 200$. The resulted concentration profile on the centerline is shown in Fig. 7 comparing with the experimental

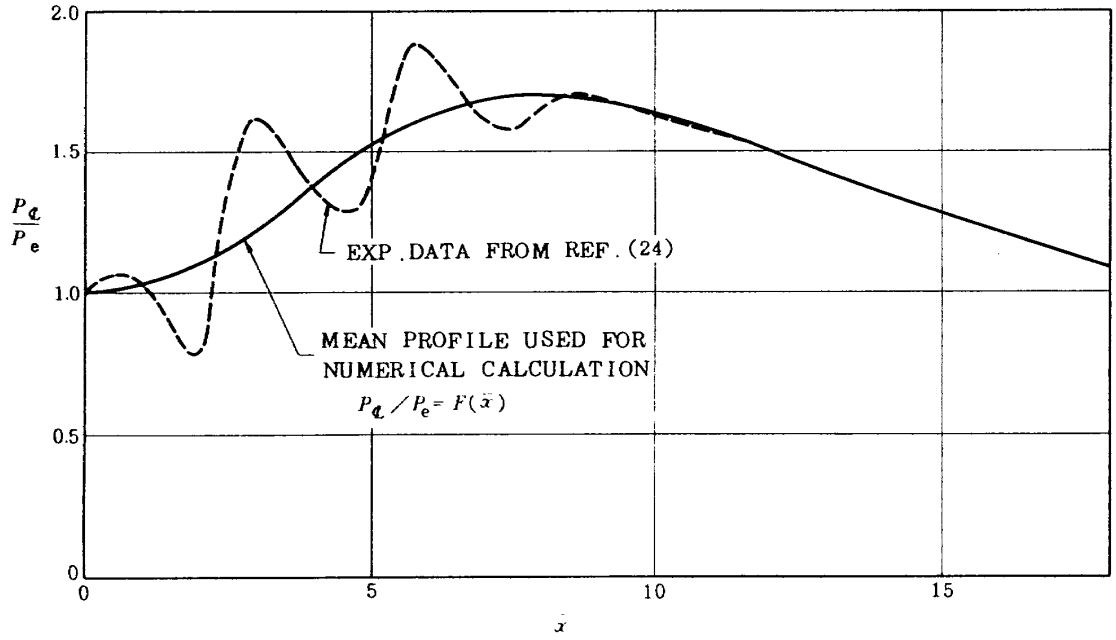


Fig. 6 Center Line Pressure Distribution (Ref. 24)

data.

From Fig. 7 it can be said that the numerical result for the centerline decay of concentration agrees well with the experimental data, and it seems that the potential core length was predicted fairly well. The calculated results for velocity and temperature on the centerline are shown in Fig. 8 within the region where the static pressure changed remarkably along the centerline. Comparing with the experimental results, the calculated profiles of velocity and temperature agree fairly well with the data within the region of $x/D_j \leq 5$, but do not for $x/D_j > 5$.

The other three models, namely Prandtl, Ferri, and Schetz eddy viscosity model, were selected to compare their numerical solutions with the present one, and it was found that any model could not predict the concentration decay on the centerline correctly as shown in Fig. 7.

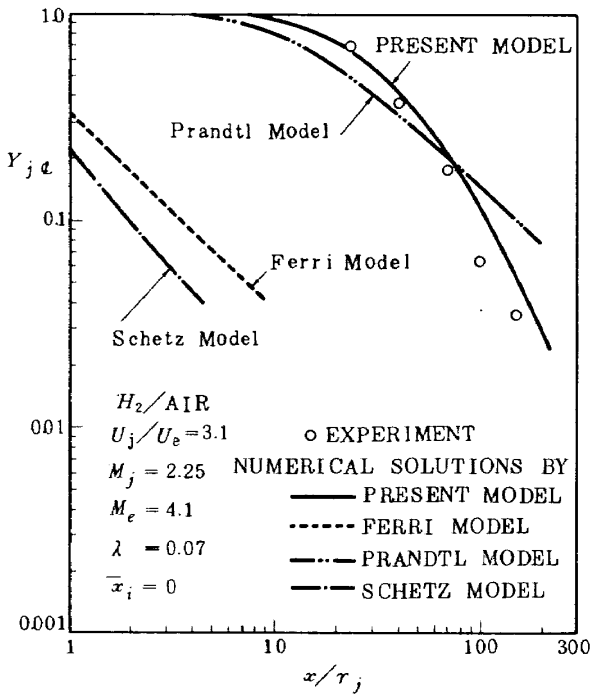


Fig. 7 Comparison of Numerical Results with the Data of Zakkay et al.(24)

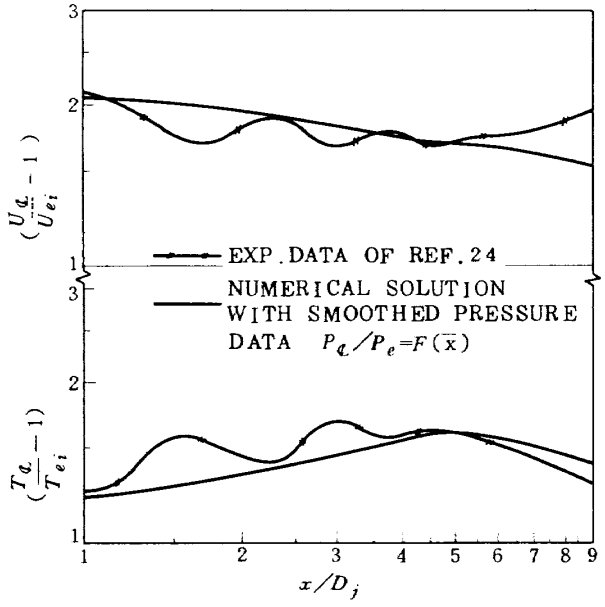


Fig. 8 Comparison of Numerical Results with the Data of Zakkay et al. (Ref. 24)

## 3. DISCUSSIONS

Being obvious from the numerical results presented in the previous section, the present diffusion model is found to provide good predictions for the turbulent jet mixing in the wide range of flow conditions without pressure gradient together with the appropriate constant values for $Pr_t$ and $Sc_t$. For the case with pressure gradient the prediction for the concentration decay is satisfactory also, however, predictions are problematic for velocity and temperature.

The reasons for the failure to predict the velocity decay could be found by the following detailed investigations for the experimental and the numerical results.

In Fig. 9 the flow pattern is made up from the pressure distribution data given in Ref. 24. At the location of $\bar{x} = 10$ the expansion and the compression waves are absorbed into the shear flow. This length of $\bar{x} = 10$ corresponds approximately to the potential core length for concentration where $Y_{j\mathcal{L}}$ starts decreasing. In this core region the pressure gradient is positive on the average and therefore, the centerline velocity decreases with oscillation as seen in Fig. 8. In this region of $x < 10$ the numerical result for velocity predicts fairly well. After the core region the calculated velocity profile shows the monotonical decrease, though the experimental data starts increasing due to the favarable pressure gradient. This discrepancy stems from the constant $Sc_t$ ($Sc_t = \epsilon/D_t$) assumed in the present calculations which implies the similar behavior of the momentum transfer to the mass diffusion; this is obvious after the fact that the calculated velocity decreases in spite of the favorable pressure gradient after when the concentration started

decaying due to mixing. From this results the conclusion is drawn that when the pressure gradient is existing, the behavior of the mass diffusion is completely different from the one of momentum transfer, and that a constant $Sc_t$ can be applied no longer.

As seen in Fig. 8 the centerline temperature is also shifted from the data in the region of $x/D_j > 5$, but the tendency is almost the same as the data and the discrepancy is not so large comparing with that for velocity. This may be explained by that both of concentration and temperature have the scalar value, but that the velocity has a vector value. Therefore it may be concluded that a constant Lewis number can be used even in the case with pressure gradient.

Now the effects of the two parameters, namely pressure gradient and initial boundary layers developed on the nozzle walls of the inner jet are investigated numerically. In Figs. 10 and 11 the numerical results of concentration, velocity, and temperature profiles are shown which are calculated for the experimental conditions of Ref. 24 with the specialized assumption of zero pressure gradient. According to these results, it has been confirmed again that the pressure gradient does not affect the concentration, though it does the velocity and temperature profiles.

In order to investigate the effect of initial boundary layer, the very thin layers on the both sides of the inner nozzle wall were assumed as shown in Fig. 12. The numerical solutions for these cases given in Figs. 10 and 11 have shown that the boundary

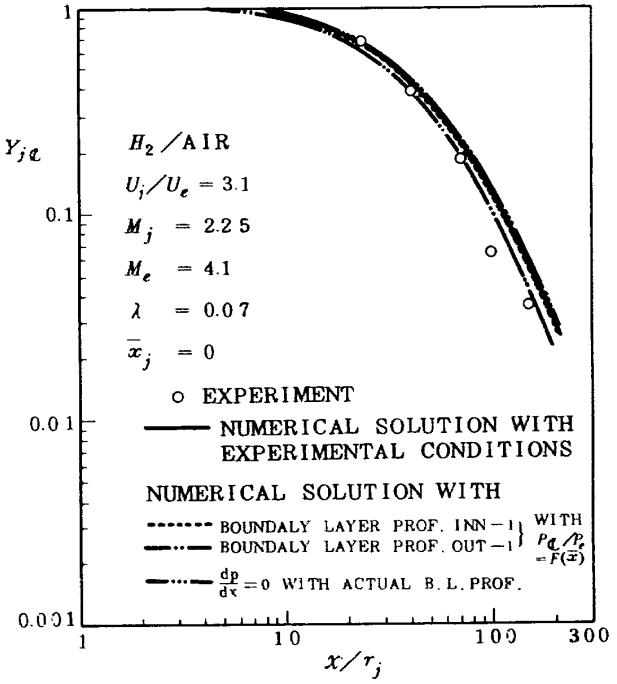


Fig. 10 Effect of Pressure Gradient and Initial Boundary Layer for Concentration, Data of Ref. 24

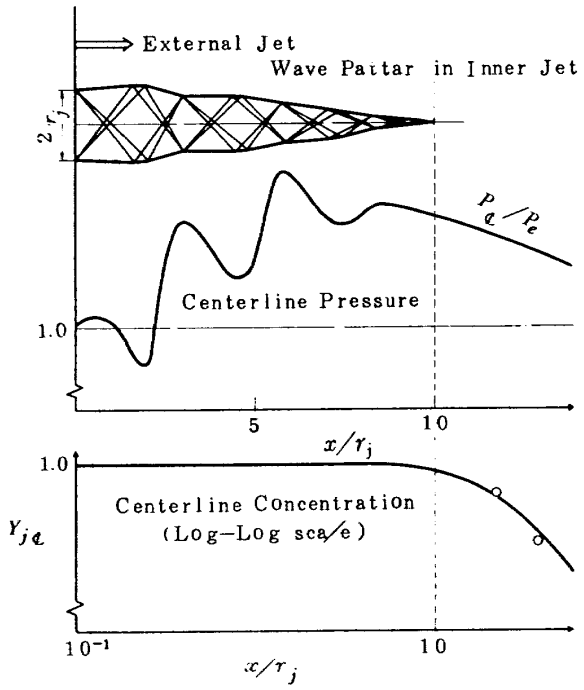


Fig. 9 Wave Pattern, Pressure Oscillation and Concentration Decay (Ref. 24)

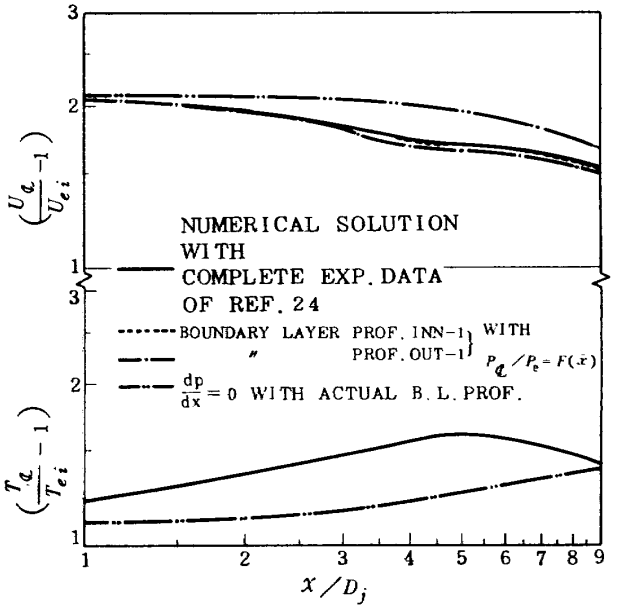


Fig. 11 Effect of Boundary Layer and Pressure Gradient

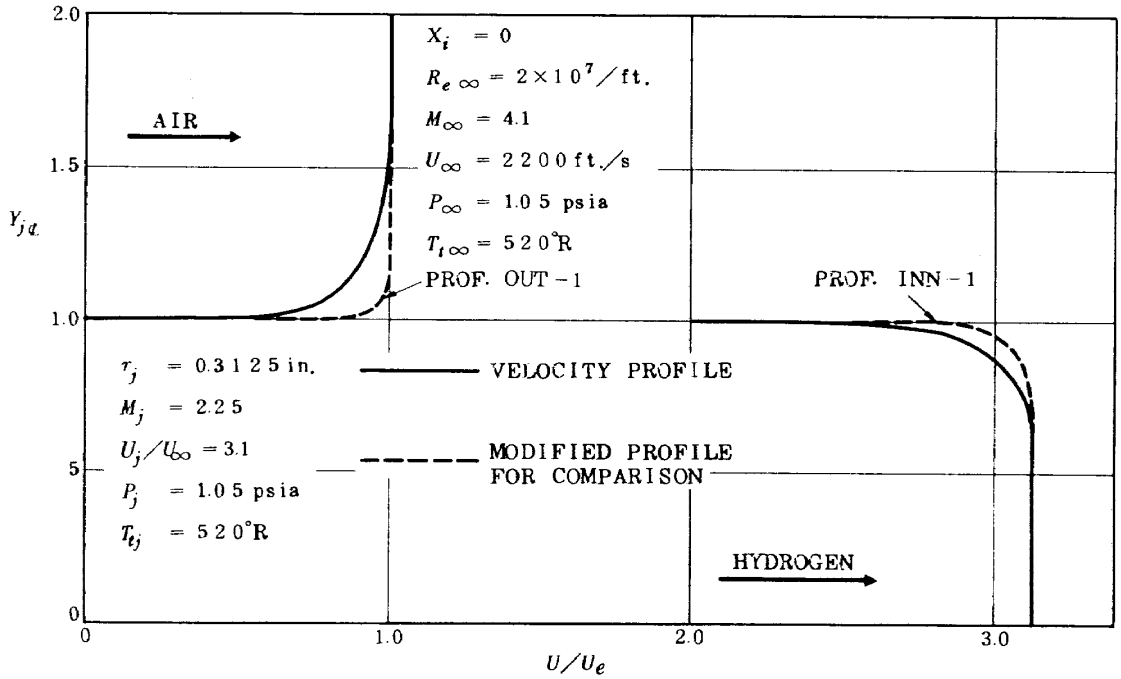


Fig. 12 Initial Boundary Layer Profiles at the Nozzle Exit; Exp. Data of Ref. (24) and The Modified for Numerical Calculation

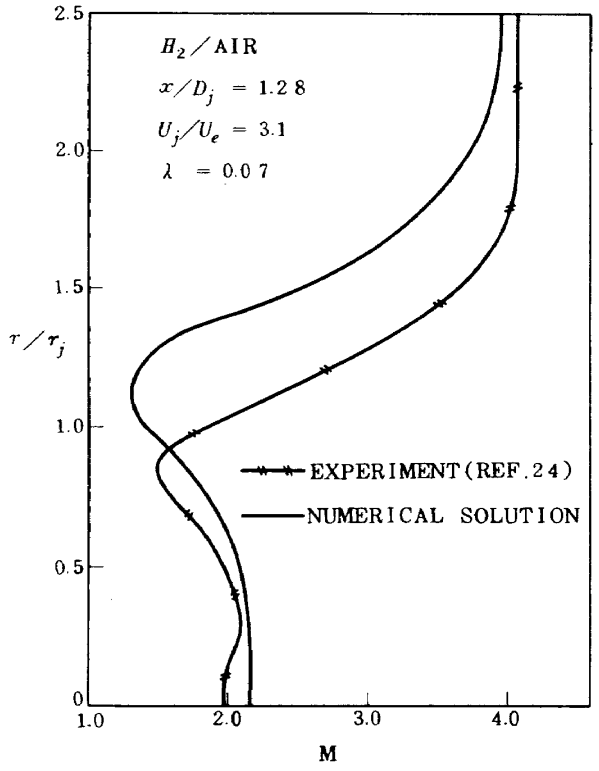


Fig. 13 (a) Comparison of Numerical Results with the Data of Zakkay et al. (Ref. 24)

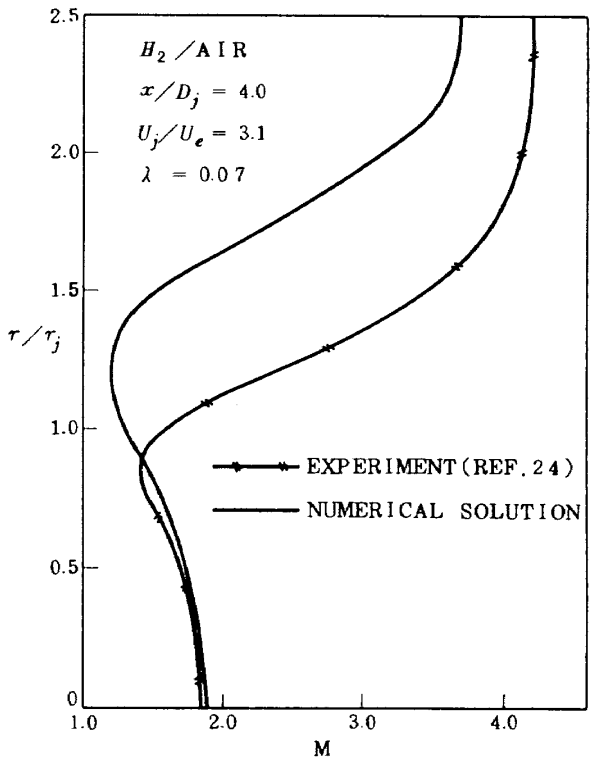


Fig. 13 (b)

layer "Profile out-1" developed on the outer side of the wall affects the concentration and velocity profile slightly, but that the "Profile inn-1" on the inner side does not affect at all. This result agrees with the experimental results obtained in Ref. 6. This may be explained by that since the density of inner hydrogen jet is very small, the difference of the initial momentum between the assumed thin layer and the actual layer on the inner side of the wall is too small to affect the mixing process significantly.

The calculated radial distributions of Mach number are shown in Figs. 13 (a) and (b) at the two stages of $\bar{x}$ = 2.56 and 8.0. Both results show the very good agreement with the experimental data within the inner nozzle radius $r \leqslant r_j$. However, in the region of $r > r_j$ there are considerable discrepancies between numerical and measured profiles. This differences are probably due to the radial pressure gtadient existing in the actual flow field as seen in Fig. 14.

## 4. CONCLUSIONS

The concluding remarks of this theoretical investigations, which are concerned to the high speed coaxial jet mixing, are drawn as follows;

(1) The turbulent diffusion coefficient is modeled by employing the solution for the liniarized species equation, which does not include any adjustable constant.

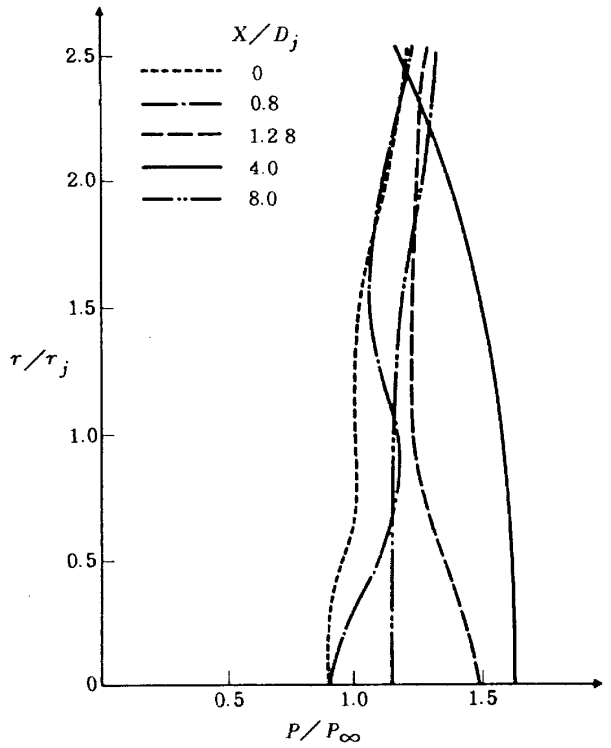


Fig. 14 Experimental Data for Radial Static Pressure Profiles (Ref. 24)

(2) Comparisons of the numerical solutions of wake equations with the experimental data have proved that the present diffusion model provides (i) for the case with large pressure gradient, the good prediction for the concentration profile on the centerline, and (ii) for the case without pressure gradient, the excellent predictions for the axial and the radial profiles both of concentration and velocity together with $Sc_t = Pr_t = 0.8$ and $Le_t = 1.0$.

(3) When the pressure gradient is existing in the mixing field, a constant Schmidt number cannot be applied, but a constant Lewis number may be applicable.

(4) According to the numerical investigations it can be said that (i) the axial pressure gradient affects the velocity and temperature profiles, but does not the concentration profile on the centerline at all. (ii) the initial boundary layer developed on the outside wall of the inner nozzle affects slightly the profiles of velocity and concentration on the centerline, but one developed on the inside wall does not affect any profile.

(5) The analytical prediction of concentration half radius given by eq. (12) agreed quite well with the data of Chriss.

(6) The initial Mach number ratio, in other words, the initial momentum ratio of both jets was found to be the governing parameter for the potential core length of concentration which was correlated well by eq. (16) for all avairable experimental data of high speed jet mixing.

(7) Any one of the eddy viscosity models suggested by Prandtl, Ferri and Schetz could not predict the data for the supersonic jet mixing with pressure gradient correctly.

## REFERENCE

[1] Ferri, A., Libby, P. A., and Zakkay, V., "Theoretical and Experimental Investigation of Supersonic Combustion," High Temperatures in Aeronautics, Pergamon Press, New York, 1962.

[2] Alpinieri, L. J., "Turbulent Mixing of Coaxial Jets, "AIAA J., 2, 9, Sept. 1964.

[3] Ting, L., and Libby, P. A., "Remarks on the

Eddy Viscosity in Compressible Mixing Flow," J. of the Aero/Space Sci., 27, Oct. 1960.

[4] Donaldson, C. duP., and Gray, K. E., "Investigation of Free Mixing of Dissimilar Gases," AIAA J., 4, 11, Nov. 1966.

[5] Peters, C. E., "Turbulent Mixing and Burning of Coaxial Streams Inside a Duct of Arbitrary Shape," AEDC TR-68-270, Jan. 1969.

[6] Zakkay, V., Krause, E., and Woo, S. D. L., "Turbulent Transport Properties for Axisymmetric Heterogeneous Mixing," AIAA J., 2, 11, Nov. 1964.

[7] Schetz, J. A., "Turbulent Mixing of a Jet in a Coflowing Streams," AIAA J., 6, 10, Oct. 1968.

[8] Clauser, F. H., "The Turbulent Boundary Layer," Advances in Applied Mech., Vol. 4, Pergamon Press, New York, 1956.

[9] Zelanzny, S. W., Morgenthaler, J. H., and Herendeen, D. L., "Reynolds Momentum and Mass Transport in Axisymmetric Coflowing Streams," Proc. of the 1970 Heat Transfer and Fluid Mech. Inst., Stanford Univ. Press, Stanford, Calif., 1970.

[10] Harsha, P. T., "Free Turbulent Mixing: A Critical Evaluation of Theory and Experiment," AEDC TR-71-36, Feb. 1971.

[11] Forstall, W., Jr., and Shapiro, A. H., "Momentum and Mass Transfer in Coaxial Gas Jets," J. of Applied Mech. 17, Dec. 1950.

[12] Chriss, D. E., "Experimental Study of the Turbulent Mixing of Subsonic Axisymmetric Gas Streams, "AEDC TR-68-133, Aug. 1968.

[13] Peters, C. E., Chriss, D. E., and Paulk, R. A., "Turbulent Transport Properties in Subsonic Coaxial Free Mixing Systems," AIAA Paper No. 69–681, June 1969.

[14] Zakkay, V., and Krause, E., "Mixing Problems with Chemical Reactions," Supersonic Flow, Chemical Process and Radiative Transfer, Pergamon Press, New York, 1964.

[15] Zakkay, V., Sinha, R., and Fox, H., "Some Remarks of Diffusion Process in Turbulent Mixing, "AIAA J. 6, 7, July 1968.

[16] Libby, P. A., "Theoretical Analysis of Turbulent Mixing of Reacting Gases with Application to Supersonic Combustion of Hydrogen," ARS J. 32, 3, March 1962.

[17] Kleinstein, G., "Mixing in Turbulent Axially Symmetric Free Jets," J. of Spacecraft, 1, 4, July–Aug. 1964.

[18] Martelluci, A., Trucco, H., Ranlet, J., and Agnon, A., "Measurements of the Turbulent Near Wake of a Cone at Mach 6," AIAA Paper 66–54, Jan. 1966.

[19] Sinha, R., and Zakkay, V., "Experimental and Theoretical Investigation of the Near Wake in an Axisymmetric Supersonic Flow with and without Base Injection," New York Univ., Dept. of Aeron. and Astron., Rept. NYU-AA-68-26, May 1968.

[20] Sinha, R., "Experimental and Theoretical Investigation of the Near Wake in an Axisymmetric Supersonic Flow with and without Base Injection," Ph. D. Thesis, 1968, New York Univ., New York.

[21] Keagy, W. R., and Weller, A. E., "A Study of Freely Expanding Inhomogeneous Jets," Proc. 1949 Heat Transfer and Fluid Mech. Inst., American Society of Mech. Eng., New York, May 1949.

[22] O'Connor, T. J., Comfort, E. H., and Cass, L. A., "Turbulent Mixing of an Axisymmetric Jet of Partially Dissociated Nitrogen with Ambient Air," AIAA J., 4, 11, Nov. 1966.

[23] Masters, J. I., "Some Applications in Physics of the P-Function," J. Chem. Physics, 23, 1955.

[24] Zakkay, V., Sinha, R., and Nomura, S., "Theoretical and Experimental Investigations of Turbulent Mixing of Supersonic Jets," Aerospace Research Lab., ARL Report, to be published.

TECHNICAL REPORT OF NATIONAL
AEROSPACE LABORATORY
TR-392T

航空宇宙技術研究所報告392T号(欧文)

昭和49年10月発行

発行所　航空宇宙技術研究所
東京都調布市深大寺町1,880
電話 武蔵野三鷹(0422)47-5911(大代表)
印刷所　株式会社　共進
東京都杉並区久我山4-1-7(羽田ビル)

Published by
NATIONAL AEROSPACE LABORATORY
1,880 Jindaiji, Chōfu, Tokyo
JAPAN